JOURNAL OF MATERIALS SCIENCE **33** (1998) 1819–1825

The examination of the fracture toughness of concretes with diverse structure

G. PROKOPSKI
Rzeszów University of Technology, 35-959 Rzeszów, Powstańców Warszawy 6, Poland
J. HALBINIAK AND B. LANGIER
Technical University of Częstochowa, 42-200 Częstochowa, Armii Krajowej 3, Poland

Examination of fracture toughness of concretes was made using Mode I (tension at bending) and Mode II (shearing) fracture. Subjected to examination were gravel and dolomite concretes in their natural states and the same concretes as made from paraffinated aggregates. Gravel and dolomite conretes with diverse water–cement (W–C) ratios were also examined. The values of the stress intensity factors, K_{Ic} and K_{IIc}, and those of fracture energy, J_{Ic} and J_{IIc}, were determined. In the case of concretes with variable W/C ratios, regression equations were also determined that described the dependence of the stress intensity factors and fracture energies on the W–C ratio. The paraffination of aggregates resulted in a considerable drop in the stress intensity factors studied as compared with those of concretes made from non-paraffinated aggregates. This drop was 34% for gravel as examined according to Mode I fracture, and 27% as examined according to Mode II fracture. For dolomite concrete drops were 19 and 28%, respectively. An increased W–C ratio caused a dramatic drop of both stress intensity factors. By addition of a super-plasticizer to the concrete mixture an evident improvement in the strength properties of both types of concrete occurred. Microstructural examinations performed have clearly confirmed the relationship between the type of aggregate used for concrete making and the microstructure of the concrete, particularly within the area of the contact layer between the aggregate and the cement paste.

1. Introduction

The strength of concrete, as traditionally understood and analysed, is compressive strength; which, though easy to evaluate, is not a perfect mechanical quantity because it evaluates only the maximum force that is carried by a concrete specimen of a specific form. Observations of failure of concrete specimens under a compressive load indicate that as increase in force often still occurs when the specimen already shows cracking, i.e. when it is already beyond its failure stage. This imperfection does not occur in the testing of concrete for fracture toughness. In this examination, the values of critical force and critical stresses are determined at the moment of dramatic propagation of the crack existing in the specimen.

In recent years, intensive research work has been undertaken aimed at determining the influence of the composition of the concrete mixture, including the type and amount of coarse aggregate, the W–C ratio and the associated character of the aggregate–cement paste interface layer, on the properties of hardened concrete. Particularly intensive investigations are focused on the properties of the interface layer, which extends by approximately 50 μm from the coarse aggregate–cement paste contact layer, and on the determination of its effect on the course of the failure process and the strength of the concrete. The existence of an interfacial layer of different microstructure from that of the cement paste beyond this layer has been confirmed by several researchers [1–4]. Studies on the effect of the interfacial layer on the mechanical properties of concrete have been conducted in recent years mainly applying the methods of fracture mechanics [5–8].

An argument still exits among researchers concerning the influence of specimen size on the obtained values of fracture mechanics quantities, such as the stress intensity factors, K_{Ic} and K_{IIc}, or fracture energy, J_{Ic} and J_{IIc}. It has been proposed that the height of test specimens subject to Mode I fracture, i.e. tension at bending, should be a minimum of 229 mm [9] or at least 50 diameters of the maximum grains of the coarse aggregate [10]. The subsequent results of works performed by different researchers [11, 12] have shown that the size of the concrete specimens to be examined does not have to be so large. It has been stated in the RILEM draft recommendation [13] that the minimum height of a bent specimen should be minimum 150 mm when using a coarse aggregate with a grain size of 25 mm and a minimum of 250 mm when coarse grained aggregate ranging in size from 25 to 50 mm is used. In this paper are presented results of examinations made according to Mode I fracture, obtained using specimen dimensions close to those recommended by RILEM [13].

2. Experimental procedure

2.1. Scope of the investigation

Results of studies are presented on the influence of an aggregate–cement paste interfacial layer and W–C ratios on the parameters of fracture mechanics as analysed according to Modes I (tension at bending) and II (shearing) fracture. The critical values of the stress intensity factors, K_{Ic} and K_{IIc}, and fracture energies, J_{Ic} and J_{IIc}, are determined.

The concrete mixtures were prepared using natural and paraffinated gravel aggregate, as well as broken dolomite aggregate and paraffinated broken dolomite aggregate. The specimens were unmoulded after 24 h and then stored under laboratory conditions for 27 days.

Of each concrete mixture (made from natural state aggregate, broken aggregate, paraffinated aggregates, and having diverse W–C ratios) five, 150 mm-edge cubic specimens were prepared for compressive strength testing, 14 prisms for testing according to Mode I fracture and 14 cubic specimens, each with two cracks, for testing according to Mode II fracture (Fig. 1).

2.2. Fracture toughness examination

The fracture toughness examination was carried out on a testing stand equipped with a Zwick PC-Software Z 7005 testing machine. During the tests, failure curves (representing the relationship between load versus displacement at the force application point) were recorded (Fig. 2). The increment of load was so chosen so that the maximum load was achieved in approximately 5 min. During the tests, measurement of an acoustic emission (AE) was conducted in an automatic manner and the results were recorded in the computer. Data of the AE counting rate were recorded within time intervals of 0.1 s. Based on the curves obtained for each specimen, the critical force, P_Q, was identified (Fig. 2).

The stress intensity factor, K_{Ic}, was calculated from the relationship [14]

$$K_{Ic} = \frac{6M_c}{B(W-a)^2}(\pi a)^{1/2}\,Y(a/W) \tag{1}$$

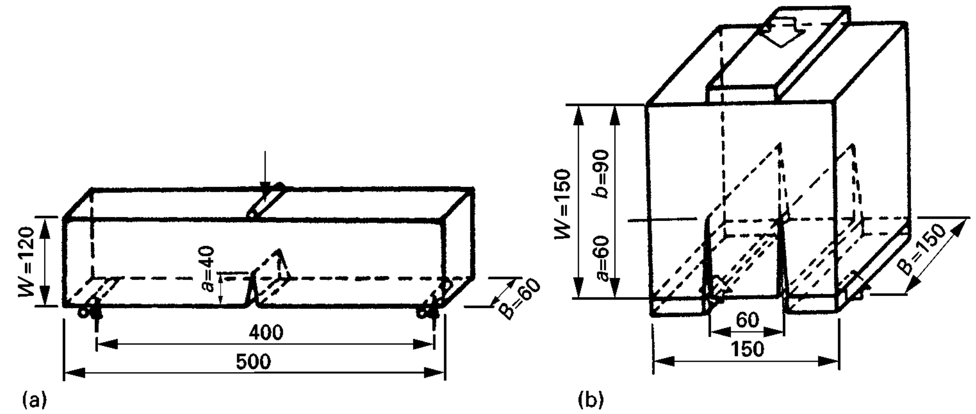

Figure 1 Schematic drawings of the specimens used in the fracture toughness examination: (a) according to Mode I, and (b) according to Mode II.

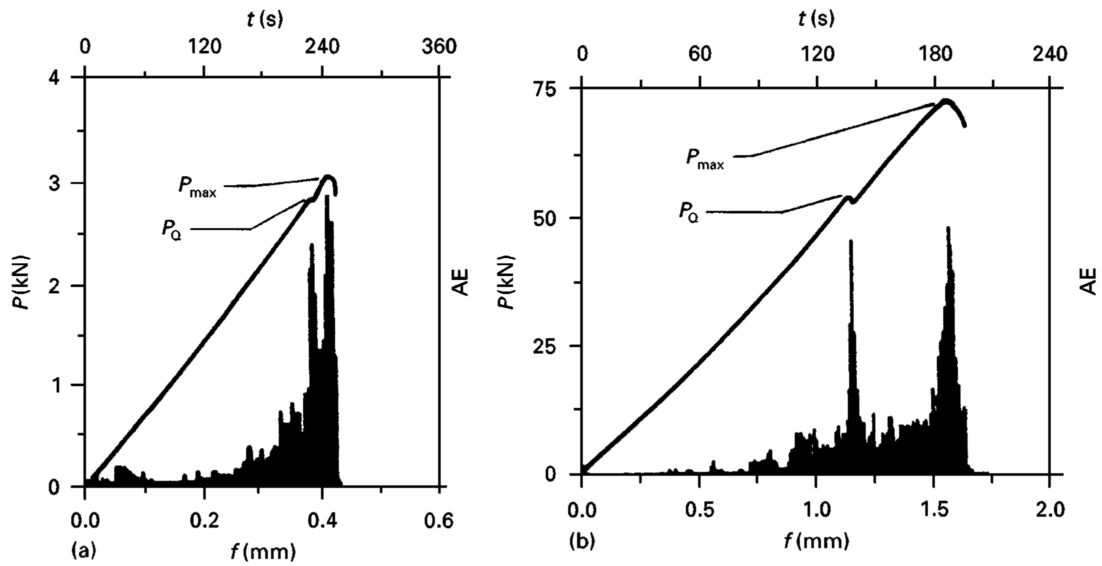

Figure 2 Examples of fracture curves and graphs of acoustic emission (AE): (a) Mode I fracture, and (b) Mode II fracture.

where M_c was the critical bending moment and $Y(a/W)$ a compliance function of the sample, determined according to Brown and Srawley [14].

The stress intensity factor, K_{IIc}, was determined according to the relationship [15]

$$K_{IIc} = \frac{5.11 P_Q}{2Bb} (\pi a)^{1/2} \tag{2}$$

where P_Q was the value of the critical force initiating the propagation of the primary crack, b the height of the specimen above the crack, B the thickness of the specimen, and a the length of the primary crack.

The energy accumulated in the specimen up to the moment of primary crack propagation was calculated by integrating the area under the failure curve. The energy was related to the area of the ligament thus determining the fracture energy, J_{Ic} or J_{IIc}

$$J_c = \frac{A}{2Bb} \tag{3}$$

where A was the energy accumulated in the specimen up to the moment of primary crack propagation, B the thickness of the specimen, and b the height of the specimen above the crack.

The results of the tests, the stress intensity factors, K_{Ic} and K_{IIc}, and the fracture energies, J_{Ic} and J_{IIc}, along with standard deviations, s, and coefficients of variation, ν, are summarized in Tables I and II.

On the basis of the results obtained, the relationships of stress intensity factors, K_{Ic} and K_{IIc} were determined as a function of the W–C ratio for gravel and dolomite concretes. In Figs 3 and 4, the respective graphs of regression equations (solid lines), confidence intervals for the regression equations, and confidence intervals for an arbitrary predicted value of a dependent variable calculated from the regression equations (dotted lines) are shown, as well as the mean values of the results from the specimen tests for pre-set W–C ratios.

2.3. Microstructural examination

The examinations were carried out using fragments of specimens from the fracture toughness tests, as taken from the area adjacent to the edge tips of the primary cracks. The observations were made using a Joel 5400 scanning microscope. Specimens to be tested were sprayed with graphite and then observed under magnifications ranging from ×35 to ×2000.

In the case of concrete made of non-paraffinated gravel aggregate (Fig. 5), small-sized discontinuities were observed at the interface between the gravel grains and the cement paste and a few microcracks within the paste itself. The gravel grains extracted from the cement paste had a smooth surface, which indicated poor adhesion of the paste to the gravel aggregate grains.

On the photographs showing the microstructures of the paraffinated gravel aggregate (Fig. 6) the occurrence of large areas of discontinuity was observed on the boundaries between the aggregate grains and the cement paste. Paraffin films formed on the aggregate grains were also observed (Fig. 7), that promoted the propagation of microcracks during the load increment.

In concrete made from non-paraffinated dolomite aggregate, fewer microcracks were observed on the boundary between the dolomite aggregate and the cement paste (Fig. 8) as compared with the gravel concrete. Exposed dolomite grains were closely coated with cement paste. On the photomicrographs of concrete made from paraffinated dolomite aggregates large discontinuities were observed at the aggregate grains and the cement paste interface (Fig. 9).

TABLE I Results of the strength tests of concretes made of aggregates in their natural state and using paraffinated aggregates

Concrete		Gravel Type		Dolomite type	
Composition of concrete mixture, kg					
Cement		322		338	
Water		140		159	
Aggregate		2003		1989	
W–C ratio		0.43		0.47	
Aggregate type		Natural	Paraffinated	Natural	Paraffinated
Compressive strength, R_c, MPa		42.5	29.5	53.7	29.6
Drop in R_c as a result of coarse aggregate paraffination, %		30.6		44.9	
Stress intensity factor	K_{Ic}, MN m$^{-3/2}$	0.67	0.44	0.82	0.66
	s, MN m$^{-3/2}$	0.06	0.05	0.05	0.03
	ν, %	9.5	11.9	5.4	5.3
	K_{IIc} MN m$^{-3/2}$	4.00	2.93	4.93	3.53
	s, MN m$^{-3/2}$	0.30	0.30	0.50	0.30
	ν, %	8.0	9.6	11.2	9.2
Drop in K_c as a result of paraffination, %	K_{Ic}	34.1		19.4	
	K_{IIc}	26.8		28.3	
Fracture energy	J_{Ic}, N m^{-1}	27.8	18.3	42.8	33.2
	s, N m^{-1}	4.6	4.6	6.0	3.5
	ν, %	16.7	25.1	14.1	10.6
	J_{IIc}, N m^{-1}	702.4	544.7	944.2	570.4
	s, N m^{-1}	102.7	110.1	173.2	77.0
	ν, %	14.6	20.2	18.3	13.5
Drop in J_c as a result of paraffination, %	J_{Ic}	34.2		22.6	
	J_{IIc}	22.5		43.7	

TABLE II Results of the strength testing of gravel and dolomite concretes with diverse W–C ratios

Gravel concrete		Series A	Series B	Series C	Series D
Composition of concrete mixture, kg					
Cement		357	357	357	357
Water		155	191	226	119
Aggregate		1911	1911	1911	1911
Plastcizer, addiment FMF		–	–	–	3.3
W–C ratio		0.43	0.53	0.63	0.33
Compressive strength, R_c, MPa		54.1	39.8	26.5	69.9
Stress intensity factor	K_{Ic}, MN m$^{-3/2}$	0.64	0.61	0.40	0.75
	s, MN m$^{-3/2}$	0.05	0.07	0.09	0.07
	ν, %	7.70	11.0	23.8	9.7
	K_{IIc}, MN m$^{-3/2}$	4.23	3.35	2.82	4.98
	s, MN m$^{-3/2}$	0.45	0.29	0.20	0.32
	ν, %	10.7	8.6	7.0	6.4
	J_{Ic}, N m^{-1}	27.2	27.1	15.3	29.9
	s, N m^{-1}	4.3	5.9	4.7	6.0
	ν, %	15.8	21.7	31.0	20.0
Fracture energy	J_{IIc}, N m^{-1}	722.4	748.9	530.8	1111.3
	s, N m^{-1}	144.0	118.1	82.4	131.6
	ν, %	19.9	15.8	15.5	11.8
Dolomite concrete					
Composition of concrete mixture, kg					
Cement		353	353	353	353
Water		166	201	236	131
Aggregate		1963	1963	1963	1963
Plasticizer, addiment BV3, % cement mass		–	–	–	0.55
W–C ratio		0.47	0.57	0.67	0.37
Compressive strength, R_c, MPa		69.6	49.5	34.3	80.1
Stress intensity factor	K_{Ic}, MN m$^{-3/2}$	0.83	0.70	0.61	0.87
	s, MN m$^{-3/2}$	0.05	0.08	0.06	0.06
	ν, %	6.3	10.9	10.3	6.4
	K_{IIc}, MN m$^{-3/2}$	4.63	4.00	3.16	5.05
	s, MN m$^{-3/2}$	0.78	0.50	0.54	0.59
	ν, %	16.8	12.5	17.1	11.7
Fracture energy	J_{Ic}, N m^{-1}	86.2	82.7	61.4	94.8
	s, N m^{-1}	10.1	18.5	19.4	21.7
	ν, %	11.7	22.4	31.5	22.9
	J_{IIc}, N m^{-1}	961.6	722.5	551.4	1118.5
	s, N m^{-1}	310.0	102.2	126.1	183.3
	ν, %	32.2	14.1	22.9	16.4

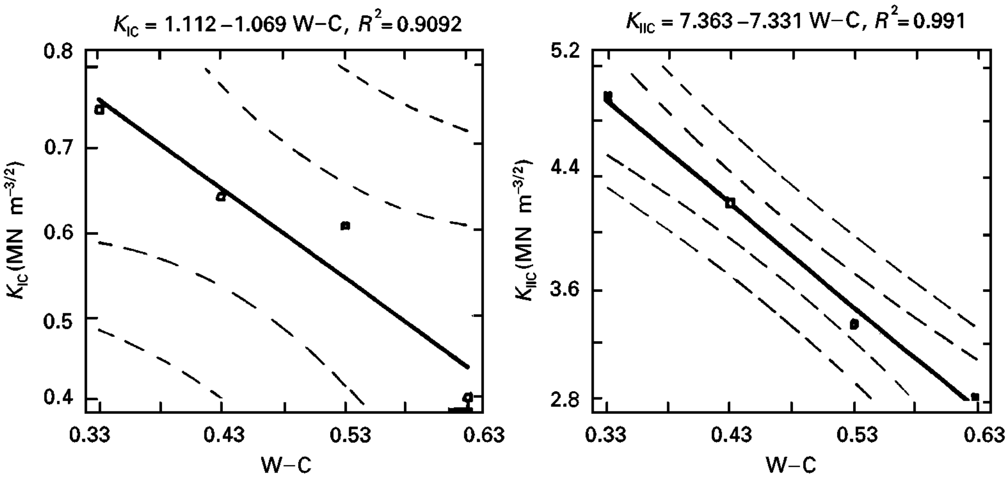

Figure 3 Dependence of K_{Ic} and K_{IIc} on W–C for gravel concrete.

In the case of gravel concrete made with a W–C = 0.43, tight filling of the structure with cement grains was observed: the grains were coated with C_3S (Fig. 10). With the increase in the amount of water in the concrete, an increase in the number of microcracks occurred within the cement paste (Fig. 11).

With the greatest amount of water added to the concrete mixture (W–C = 0.63), characteristic needle-shaped etringite forms were observed, that caused increased porosity of the concrete (Fig. 12). Addition of a plasticizer to the concrete mixture of lowered water content (W–C = 0.33) resulted in the formation

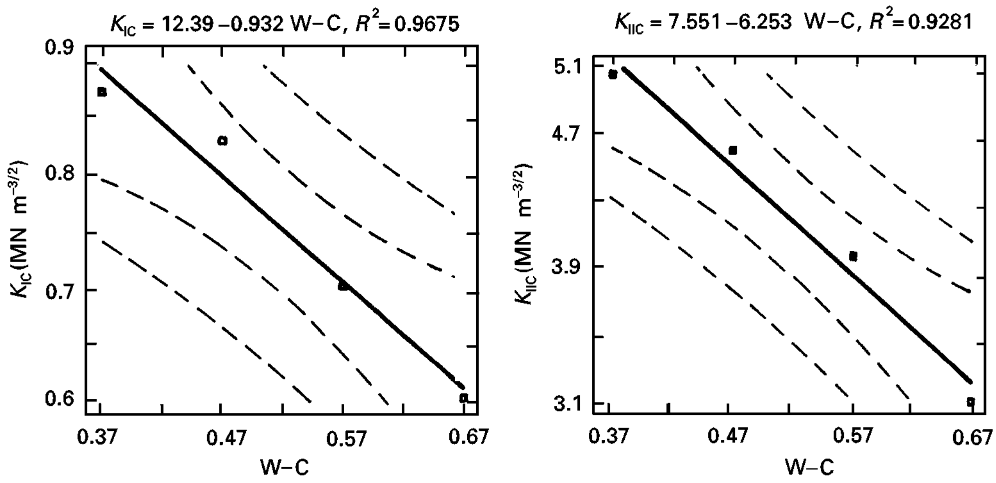

Figure 4 Dependence of K_{Ic} and K_{IIc} on W–C for dolomite concrete.

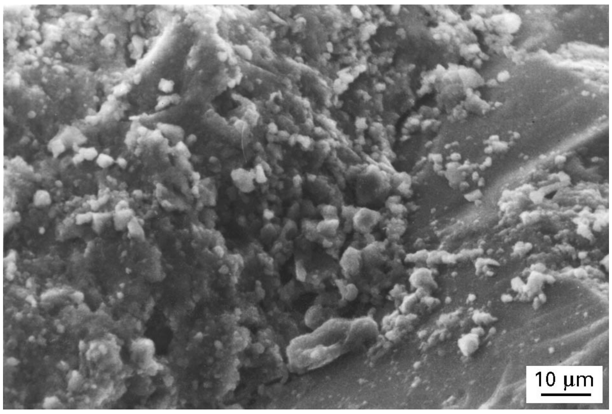

Figure 5 Microstructure of concrete made of non-paraffinated gravel aggregate (microcracks are visible at the interface between the gravel grains and the cement paste, and in the cement paste itself).

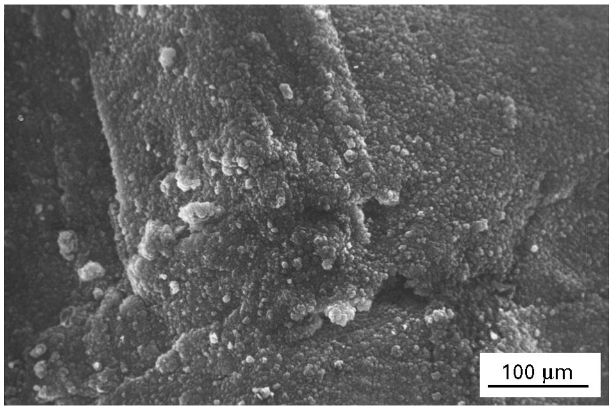

Figure 7 Microstructure of concrete made from paraffinated gravel aggregate (a paraffin film is visible on the gravel grain).

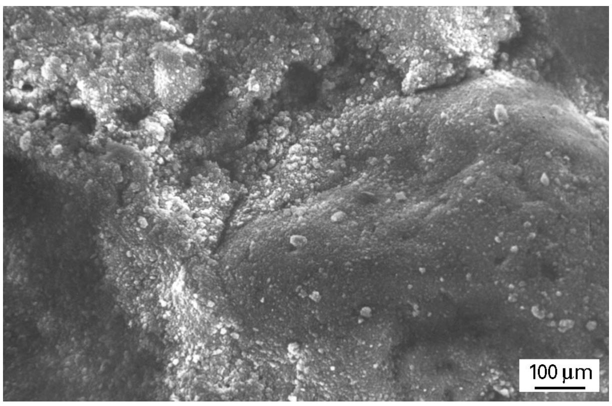

Figure 6 Microstructure of concrete made from paraffinated gravel aggregate (discontinuity is visible on the grain and cement paste boundary).

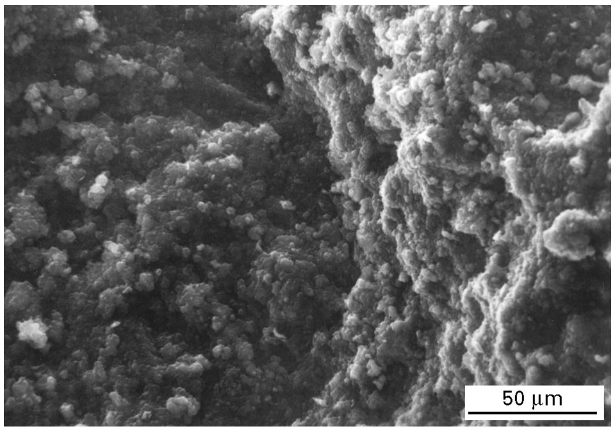

Figure 8 Microstructure of concrete made from non-paraffinated gravel aggregate (a microcrack is visible at the aggregate–cement paste interface, i.e. on the left of the photograph).

of a "compact" cement paste structure with fine and well developed C_3S grains coating the cement grains (Fig. 13).

In the case of concrete made from dolomite aggregate, with increasing water content, increasingly large discontinuities were observed at the interface between the dolomite aggregate grains and the cement paste (Figs 14 and 15). Addition of a super-plasticizer to the concrete mixture (W–C = 0.37) resulted in the formation of a compact cement paste structure, that closely filled up the interface with aggregate grains. In this case (Fig. 16) small discontinuities were

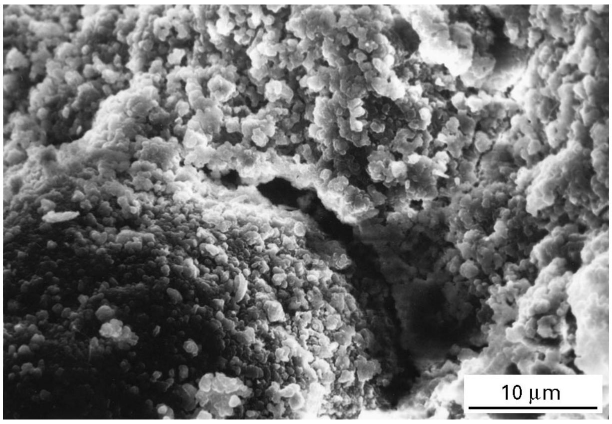

Figure 9 Microstructure of concrete made from paraffinated gravel aggregate (a large-sized microcrack is visible at the aggregate and cement paste interface).

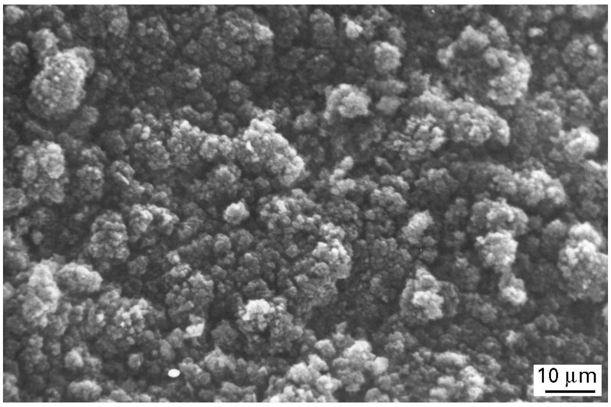

Figure 10 Microstructure of gravel concrete for W–C = 0.43 (the structure is closely filled up with cement grains coated with C_3S).

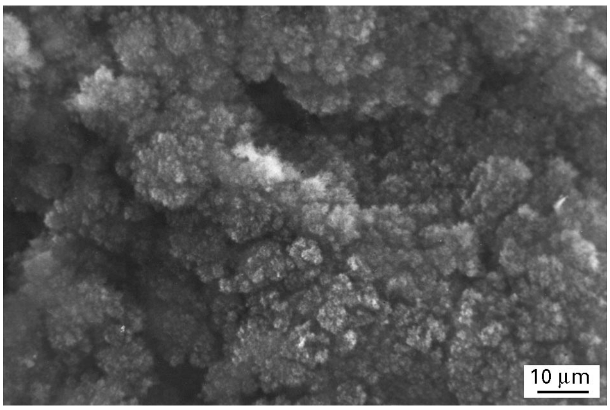

Figure 11 Microstructure of gravel concrete for W–C = 0.53 (increased porosity and microcracks are visible).

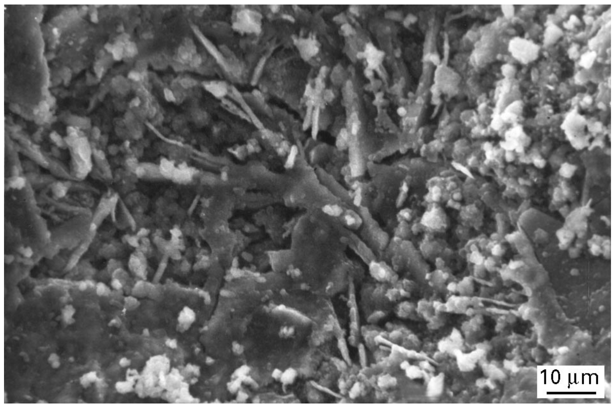

Figure 12 Microstructure of gravel concrete for W–C = 0.63 (characteristic needle-shaped forms of etringite are visible).

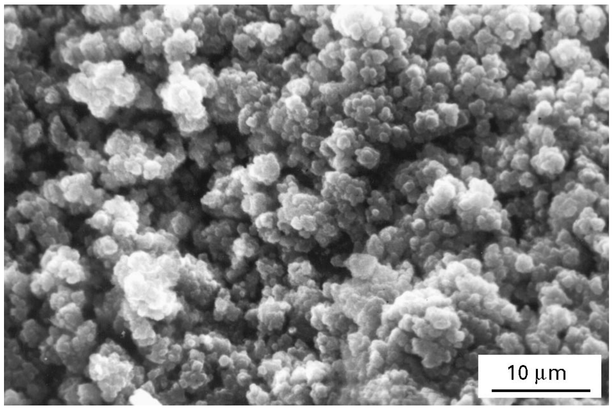

Figure 13 Microstructure of gravel concrete for W–C = 0.33 (tight filling of the structure with cement grains coated with C_3S is seen).

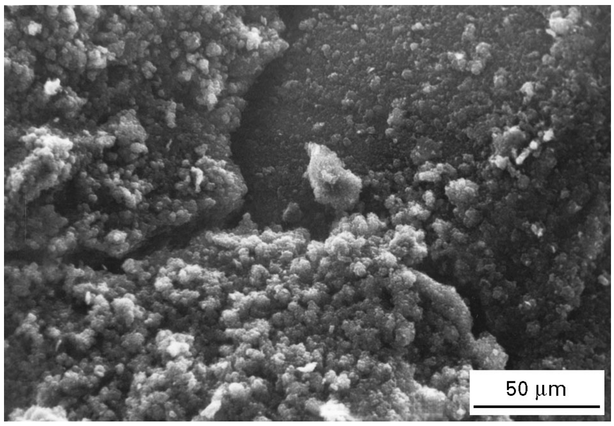

Figure 14 Microstructure of dolomite concrete for W–C = 0.57 (clear discontinuity is visible at the aggregate and cement paste interface and a microcrack is seen in the cement paste).

visible at the aggregate and cement paste interface, as well as microcracks in the paste, that were situated perpendicular to the dolomite grains.

3. Conclusions

The investigations have shown that covering the gravel aggregate grains with paraffination results in a drop of K_{Ic} by approximately 34% in relation to concrete made from non-paraffinated aggregate. A similar dependence has been found in Mode II fracture studies. In this case, the drop in K_{IIc} was 27%. Paraffination of the dolomite aggregate grains causes a 19% drop in the K_{Ic} value and a 28% drop in the K_{IIc} value.

With increasing W–C ratio, a dramatic drop in both stress intensity factors, K_{Ic} and K_{IIc}, took place. Particularly evident in this case was a decrease in K_{IIc}, that indicated the great sensitivity of concrete to shearing stresses.

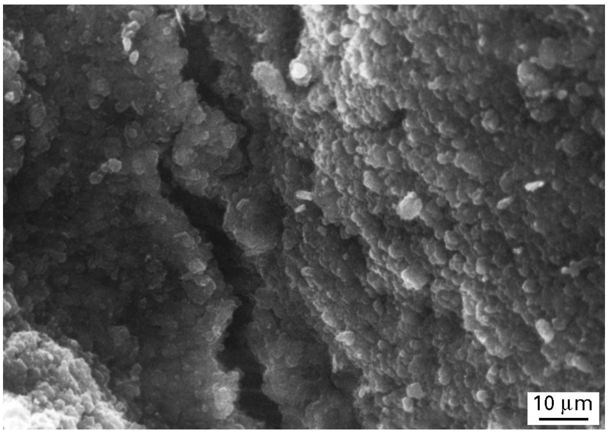

Figure 15 Microstructure of dolomite concrete for W–C = 0.67 (a large discontinuity is visible in the cement paste beyond the paste and dolomite grain contact line).

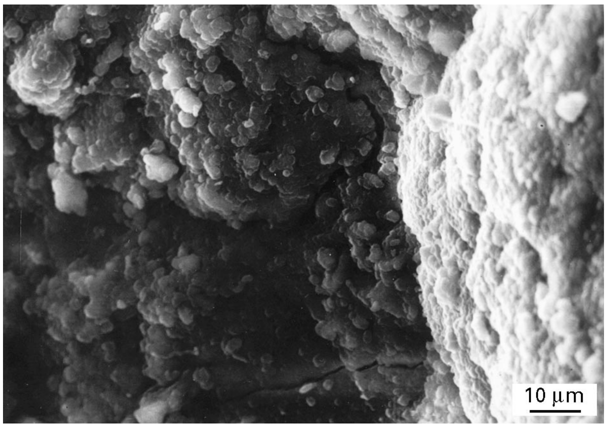

Figure 16 Microstructure of dolomite concrete containing a plasticizer for W–C = 0.37 (no evident discontinuities at the aggregate grain and cement paste interface are seen, and microcracks are visible in the cement paste, situated perpendicular to the dolomite grain).

An increase in W–C caused an increasing number of pores and microcracks to be observed. The formation of needle-shaped forms of etringite resulted in "loosening" of the structure, and promoted the propagation of primary cracks.

By addition of a plasticizer to the concrete, considerable improvement in the concrete structure was obtained. The structure was the most "compact" and showed the least porosity.

The use of larger specimens with dimensions as recommended by RILEM [13] did not lead to any significant changes in the values of K_{Ic} obtained in comparison with those of smaller specimens used previously for the same purpose [5]. This supports the argument that has been accepted recently by many researchers, which says that the size of the concrete specimens for the determination of critical stress intensity factors does not have to be excessively large.

References

1. J. W. CHATERJI and J. W. JEFFERY, *Indian Concr. J. August* **45** (1971) 346.
2. H. KAWAKAMI, in International RILEM Conference on interfaces in cementitious composites, Toulouse 21–23 October 1992. (Spon, London, 1993) pp.179–86.
3. K. MITSUI, LI ZONGJIN, D. A. LANGE and S. P. SHAH, *ibid* pp. 119–28.
4. P. SIMEONOV and S. AHMAD, *Cement Concr. Res.* **25** (1995) 165.
5. G. PROKOPSKI. *Arch. Inż. Ląd.* **35** (1989) 349 (in polish).
6. *Idem*, in Proceedings of the International Symposium on brittle matrix composites IV, edited by A. M. Brandt, V. C. Li and I. H. Marshall, Warszawa, 13–15 September 1994 (Woodhead, Cambridge-Warsaw, 1994) 475.
7. A. BOCHENEK and G. PROKOPSKI, *Arch. Inż. Ląd.* **34** (1988) 261 (in polish).
8. M. G. ALEXANDER, in Proceedings of the International RILEM Conference on interfaces in cementitious composites, Toulouse 21–23 October 1992 (Spon, London, 1993) pp. 129–37.
9. P. F. WALSH. *Indian Concr. J.* **46** (1972) 469.
10. Z. P. BAŽANT, *J. Eng. Mech. Div. ASCE* **110** (1984) 518.
11. W. BRAMESHUBER, "Bruchmechanische eigenschaften von jungem beton," Schrifttenreihe des Instituts fur Massivbau und Baustoffechnologie, Universitat Karlsruhe, Heft 5 (1988).
12. W. BRAMESHUBER and H. K. HILSDORF, *Eng. Frac. Mech.* **35** (1990) 95.
13. RILEM Draft Recommendations, "TC-89 FMT fracture mechanics of concrete–test methods, materials and structures," vol. 23 (RILEM, 1990).
14. W. F. BROWN Jr. and J. E. SRAWLEY, ASTM STP 410 (1967).
15. J. WATKINS, *Int. J. Fract.* **23** (1983) K135.

Received 15 November 1996
and accepted 5 December 1997